Synthesis of Ruthenium Dioxide−Titanium Dioxide Aerogels: Redistribution of Electrical Properties on the Nanoscale

Karen E. Swider,[†,§] Celia I. Merzbacher,*[,‡] Patrick L. Hagans,[†] and Debra R. Rolison*[,†]

Code 6170 and Code 5612, Naval Research Laboratory, Washington, D.C. 20375

Received December 6, 1996. Revised Manuscript Received February 20, 1997[⊗]

High-surface area RuO_2−TiO_2 is an important material for catalytic and power source technologies. To create this mixed oxide as a nanoscale, high-surface-area material, we have synthesized electrically conductive aerogels of $Ru_nTi_{1-n}O_x$ via sol−gel chemistry and supercritical drying of the resulting gel. The structural and electrical properties of these aerogels are characterized after annealing using X-ray diffraction, X-ray photoelectron spectroscopy, surface-area measurements, and impedance spectroscopy. Their properties are affected by the nature of the $RuCl_3$ precursor and the initial sol-gel chemistry. Whereas bulk 32 mol % RuO_2·TiO_2 is an electronic conductor, a dominant ionic response is measured in the impedance of $Ru_{0.32}Ti_{0.68}O_x$ aerogels. This impedance is ascribed to a proton conduction mechanism associated primarily with the hydrous surface of the RuO_x component. The electrical conductivity of these $Ru_{0.32}Ti_{0.68}O_x$ aerogels at 25 °C increases from 10^{-4} S cm^{-1} in ambient air to 10^{-2} S cm^{-1} under an increased partial pressure of water, which is characteristic of a protonic conductor. The electronic conductivity of these aerogels improves with exposure to dry oxygen, which is consistent with the oxidation of Ru^{3+} surface defects. Synthesizing RuO_2−TiO_2 as an aerogel—i.e., as high-surface-area, networked interface—accentuates the surface properties of this material. The electrical (electronic + protonic) transport properties of bulk RuO_2−TiO_2 are redistributed when synthesized as an aerogel. Whereas electronic transport dominates the characteristics of the dense form, the protonic transport of the hydrous oxide surfaces governs the electrical properties of the aerogel. Aerogels provide a useful means to isolate, study, and control the surface of metal oxides.

Introduction

Electrically conductive transition-metal oxides are materials of fundamental relevance to catalysis and in power sources.[1−6] These applications require high-surface-area materials with defective or charged surfaces which facilitate ion- and/or electron-transfer reactions. In this paper, we describe the synthesis and characterization of high-surface-area, low-density aerogels of ruthenium dioxide−titanium dioxide, and we discuss the relationship between their nanoscale structure and their electrical properties.

Pure RuO_2 is a metallic conductor due to a d-band conduction mechanism.[7] Single crystals of anhydrous RuO_2 exhibit conductivity on the order of 10^4 S cm^{-1},[8] despite an oxygen deficiency[9,10] which is charge compensated by Ru^{3+} defects in the lattice.[10] Anhydrous RuO_2 is used as a thick-film resistor,[11] but the hydrous oxide is preferred in electrocatalysis.[3] Although this electrochemically active oxide has protons on its surface,[3,12] it is called RuO_2 by convention. RuO_2 electrodes are typically prepared by the thermal decomposition of $RuCl_3$·yH_2O, producing materials which are hydrous and more correctly described as RuO_x·yH_2O or RuO_x-H_y.[3,12] The conductivity of a 25−40% dense pellet of RuO_2·yH_2O ($y \approx 1.3$) is ~1 S cm^{-1}.[13]

RuO_2 is mixed with TiO_2 to make electrodes for use in electrocatalysis, particularly as a dimensionally stable anode for the production of chlorine gas from brine.[3] Some electronic conduction remains as long as there is a percolation path for the d electrons in the RuO_2, so up to 85 mol % of an insulating TiO_2 component can be added to the RuO_2 to reduce the cost of the electrodes.[3,14] Although the RuO_2−TiO_2 system does not

† Code 6170.
‡ Code 5612.
§ Current address: McNeil Consumer Products, 7050 Camp Hill Road, Fort Washington, PA 19034.
* To whom correspondence may be addressed [e-mail: rolison@nrl.navy.mil; merzbacher@nrl.navy.mil].
⊗ Abstract published in *Advance ACS Abstracts,* April 1, 1997.

(1) Bond, G. C. *Heterogeneous Catalysis: Principles and Applications*, 2nd ed.; Oxford University Press: New York, 1987.
(2) Colomban, P., Ed. *Proton Conductors: Solids, Membranes and Gels—Materials and Devices*; Cambridge University Press: Cambridge, 1992.
(3) Trasatti, S. *Electrochim. Acta* **1991**, *36*, 225 and references therein.
(4) Conway, B. E. *J. Electrochem. Soc.* **1991**, *138*, 1539.
(5) Rees, A. L. G. *Chemistry of the Defect Solid State*; John Wiley: New York, 1954; p 116.
(6) Huggins, R. A.; Prinz, H.; Wohlfahrt-Mehrens, M.; Jorissen, L.; Witschel, W. *Solid State Ionics* **1994**, *70/71*, 417.
(7) Goodenough, J. B. *Prog. Solid State Chem.* **1971**, *5*, 145.
(8) Schafer, H.; Schneidereit, G.; Gerhardt, W. *Z. Anorg. Allg. Chem.* **1963**, *319*, 372.
(9) Gutbier, A. *Z. Anorg. Chem.* **1916**, *96*, 182.
(10) Cotton, F. A.; Wilkinson, G. *Advanced Inorganic Chemistry*, 2nd ed.; Wiley-Interscience: New York, 1966; p 984.
(11) Iles, G. S.; Collier, O. N. *Platinum Met. Rev.* **1967**, *11*, 126.
(12) Battaglin, G.; Carnera, A.; Della Mia, G. *J. Chem. Soc., Faraday Trans.* **1985**, *81*, 2995.
(13) Fletcher, J. M.; Gardner, W. E.; Greenfield, B. F.; Holdoway, M. J.; Rand, M. H. *J. Chem. Soc. A* **1968**, 653.
(14) Gerrard, W. A.; Steele, B. C. H. *J. Appl. Electrochem.* **1978**, *8*, 417.

S0897-4756(96)00622-9 CCC: $14.00

Table 1. Reactant Ratios for the Preparation of Ruthenium−Titanium Dioxide and Titanium Dioxide Gels and the Observed Time for Gelation

	(Ru+Ti):H_2O:H^+:EtOH/mol	Ti(O^iPr)$_4$/mL	EtOH/mL	9.1 wt % $RuCl_3$ in EtOH/g[a]	HNO_3/g	H_2O/g	gelation time/s[b]
gel A	1:6:0.08:20	1	1	4	0.033	0.505	70
gel B	1:6:0.12:20	1	1	4	0.050	0.500	45
gel C	1:4:0.08:20	1	1	4	0.033	0.330	600
gel D	1:4:0.12:20	1	1	4	0.050	0.325	480
TiO_2	1:3:0.08:20	1	2	0	0.024[c]	0.174[c]	210

[a] All (Ru−Ti)O_x samples were prepared with $RuCl_3$ [Alfa] as the Ru precursor. [b] The gelation time is for the specific sample listed, but multiple samples prepared with the chemistries listed for each class of gels yielded comparable (±10%) gelation times. [c] HNO_3 and H_2O were added to 1.57 g of 100% ethanol.

form a solid solution, TiO_2 affects the electrocatalytic properties of RuO_2.[15] Because of the electrocatalytic nature of RuO_2−TiO_2 electrodes, their surface area is critical to their performance. High-surface-area electrode materials are also important in supercapacitors or pseudocapacitors. RuO_2 acts as a pseudocapacitor, contributing both double layer and Faradaic charge, and can generate a specific capacitance as high as 720 F/g.[16] The large specific capacitance of RuO_2 makes a high-surface-area formulation of this material a prime candidate for energy storage.[4,16]

Aerogels are composites of being and nothingness, comprised of a network of nanoscale domains surrounded by a large volume fraction of mesoporosity.[17−20] These materials are of current interest in catalysis[21−23] because of their high surface areas (100−1000 m^2/g) and their mesoporosity, which can enhance the mass transport of reactant to and product molecules away from the interior nanoscale catalytic domains. Aerogels are prepared via a sol−gel process, whereby metal alkoxide precursors undergo controlled hydration and condensation reactions in an excess of solution to form a highly porous gel network.[19,24−26] The sol−gel chemistry necessary to produce aerogels differs from that used to make dip- or spin-coated thin films, because the former requires a gel network of metal−oxide bonds to form, while the latter can be obtained with a viscous sol. The gel's porosity, defined by the free volume of solvent in the gel, is retained by drying under supercritical conditions. Aerogel structures can be made up to 99% porous.[17−23]

The physicochemical properties of aerogels are altered significantly by changes in the density and the structure of the gel which in turn are defined by the sol−gel chemistry. The structure of the gel is a function of the rate of polymerization of the alkoxides, which depends on the nature of the metal alkoxide and hydrolysis catalyst[19,24−26] and on physical and chemical processing parameters.[19,25] As a result there is enormous opportunity to vary the gel but also considerable difficulty in control and reproducibility. The preparation of aerogels is further complicated when there is more than one metal alkoxide in the system because of the different reactivities of each precursor.

While SiO_2 is the most extensively studied form of aerogel, many transition-metal oxides have also been made as aerogels.[21−24,27] Recent work has focused on vanadium pentoxide aerogels[28−32] in order to create a high-surface-area electrical conductor capable of electrochemically driven lithium-ion intercalation. Increased Li^+ capacity per intercalation center is key to improving lithium batteries. In electrodes prepared with the V_2O_5-based aerogel, Li^+ capacity per mole of V_2O_5 has been found to be greater than that obtained for bulk V_2O_5 powders or V_2O_5-based xerogels.[28,29,32−34]

We have synthesized aerogels comprised of ruthenium dioxide−titanium dioxide [(Ru−Ti)O_x] to examine the effect of enhanced surface area on electrical properties. The mixed (Ru−Ti)O_x system adds a new composition to the class of electrically conductive oxides expressed as aerogels. Because fully substituted ruthenium alkoxides are not available,[35] we selected anhydrous $RuCl_3$ refluxed in ethanol as a readily accessible precursor to prepare our gels. We examined different sol−gel chemistries by varying the water and acid concentrations used in the gel preparation. These gels are supercritically dried to form aerogels and then annealed under different atmospheres and temperatures. The electrical (i.e., ionic + electronic) transport properties of the resulting nanoscale mesoporous materials are correlated to their structural and physical attributes.

Experimental Procedures

Preparation of (Ru−Ti)O_x Aerogels. We prepared mixed (Ru−Ti)O_x aerogels by modification of a recipe for titanium dioxide (TiO_2) aerogels.[36] Titanium(IV) isopropoxide (Ti(O^iPr)$_4$, Aldrich) and anhydrous $RuCl_3$ (Alfa or Aldrich) are used as precursors. A single preparation procedure is used to make aerogels with different molar ratios of Ru, H_2O, and H^+; the

(15) Burrows, I. R.; Denton, D. A.; Harrison, J. A. *Electrochim. Acta* **1978**, *23*, 493.
(16) Zheng, J. P.; Cygan, P. J.; Jow, T. R. *J. Electrochem. Soc.* **1995**, *8*, 2699.
(17) Kistler, S. S. *Nature* **1931**, *127*, 131.
(18) Fricke, J. *J. Non-Cryst. Solids* **1988**, *100*, 169.
(19) Brinker, C. J.; Scherer, G. W. *Sol-Gel Science: The Physics and Chemistry of Sol-Gel Processing*; Academic Press: San Diego, 1990.
(20) Hrubesh, L. *Chem. Ind.* **1990**, *Dec 17*, 824−827.
(21) Pajonk, G. M. *Appl. Catal.* **1991**, *72*, 217.
(22) Ko, E. I. *Chemtech* **1993**, *23*, 31−36.
(23) Schneider, M.; Baiker, A. *Catal. Rev.−Sci. Eng.* **1995**, *37*(*4*), 515.
(24) Livage, J.; Henry, M.; Sanchez, C. *Prog. Solid State Chem.* **1988**, *18*, 259.
(25) Hench, L. L.; West, J. K. *Chem. Rev.* **1990**, *90*, 33.
(26) Corriu, R. J. P.; Leclercq, D. *Angew. Chem., Int. Ed. Engl.* **1996**, *35*, 1420.
(27) Livage, J.; Sanchez, C. *J. Non-Cryst. Solids* **1992**, *145*, 11.
(28) Le, D. B.; Passerini, S.; Tipton, A. L.; Owens, B. B.; Smyrl, W. H. *J. Electrochem. Soc.* **1995**, *142*, L102.
(29) Le, D. B.; Passerini, S.; Guo, J.; Ressler, J.; Owens, B. B.; Smyrl, W. H. *J. Electrochem. Soc.* **1996**, *143*, 2099.
(30) Chaput, F.; Dunn, B.; Fuqua, P.; Salloux, K. *J. Non-Cryst. Solids* **1995**, *188*, 11.
(31) Wong, H. P.; Dunn, B.; Salloux, K.; Chaput, F.; Breiter, M. W. *Thin-Film Solid Ionic Devices and Materials*; Bates, J. B., Ed.; Electrochemical Society: Pennington, NJ, 1996; *95-22*, pp 46−51.
(32) Salloux, K.; Chaput, F.; Wong, H. P.; Dunn, B.; Breiter, M. *J. Electrochem. Soc.* **1995**, *142*, L191.
(33) Baddour, R.; Pereira-Ramos, J. P.; Messina, R.; Perichon, J. *J. Electroanal. Chem.* **1991**, *314*, 81.
(34) Tipton, A. L.; Passerini, S.; Owens, B. B.; Smyrl, W. H. *J. Electrochem. Soc.* **1996**, *143*, 3473.
(35) Bergman, R. G. *Polyhedron* **1995**, *14*, 3227.
(36) Dagan, G.; Tomkiewicz, M. *J. Phys. Chem.* **1993**, *97*, 12651.

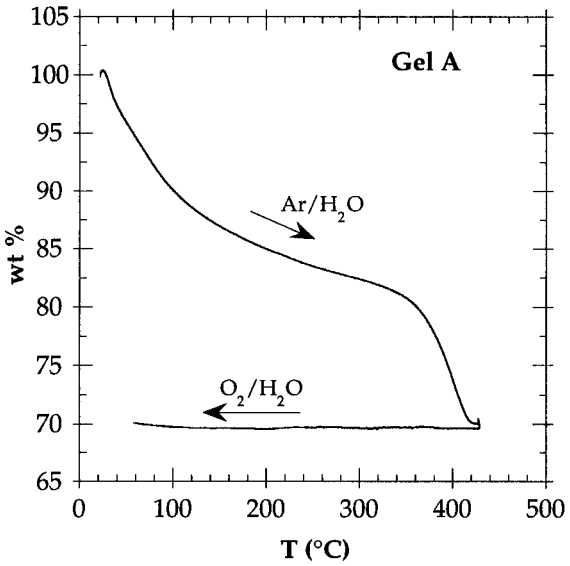

Figure 1. TGA of gel A while heating under Ar/H_2O to 425 °C at 2 °C/min and cooling under O_2/H_2O.

reactant ratios used to make the $(Ru-Ti)O_x$ aerogels for this study are shown in Table 1.

A solution of 9.1 wt % $RuCl_3$ in as-received[37] absolute ethanol (Warner-Graham) is refluxed in air for 2 h. The color of the solution after refluxing varies from green to greenish-brown, depending on the $RuCl_3$ used, as discussed below. After cooling, the appropriate amount of supernatant from the refluxed $RuCl_3$/ethanol solution is mixed with concentrated HNO_3 (Ultrex II, Baker Analyzed) and 18 MΩ cm H_2O (Barnstead Nanopure). Separately, an equivalent amount of $Ti(O^iPr)_4$ and absolute ethanol are mixed under a dry N_2 atmosphere. The Ru solution is then added rapidly to the Ti solution in the open air with stirring. This final mixture is divided into 5-mL polypropylene vials (Wheaton Omni-Vial) which are sealed using Parafilm. The sol forms a gel in times varying from less than 1 min to 3 h.

The wet gels are aged for 5 days in the vials to allow further polycondensation reactions to strengthen the gel network. During this time, the gels turn brown and excrete ca. 0.1 mL of a clear liquid. The amount of this extract increases with increasing water concentrations in the initial sol. The gels are removed from the vials and washed four times over 4 days in an excess of acetone to replace the alcohol−water pore liquid with a CO_2-miscible liquid. To form the aerogels, the acetone-washed gels are flushed with liquid CO_2 and dried under supercritical CO_2 in a critical point drying apparatus (Fisons Instruments Bio-Rad E3000).

Annealing of $(Ru-Ti)O_x$ Aerogels. The aerogels are annealed to transform them from mixed polymers of metal oxides, alkoxides, and chlorides to $(Ru-Ti)O_x$. The annealing conditions are chosen based on the weight loss−temperature profile of the residual alkoxides and chlorine, as determined by thermogravimetric analysis (TGA, TA Instruments Model 951) of the aerogels. The TGA results are specific to the aerogel composition,[38] annealing atmosphere, and heating rate.

The $(Ru-Ti)O_x$ aerogels discussed in this paper have all been processed using the following optimized heat treatment. On the basis of the TGA data shown in Figure 1, the gels are heated in an alumina boat in a 1-in. diameter quartz tube to 410 °C at 2 °C/min under Ar/H_2O flowing at ∼300 cm^3/min. The Ar is humidified by bubbling through H_2O at room temperature using a fritted gas dispersion tube, which yields gas with a relative humidity of 70−80%. The sample is held at 410 °C for 5 min and then cooled at 2 °C/min under humidified O_2 (∼300 cm^3/min). Because temperature differences as small as 10−20 °C markedly affect the final electrical properties of our aerogels, the actual furnace temperature is measured with an independent K-type thermocouple located within 1 cm of the sample.

Physical Characterization of $(Ru-Ti)O_x$ Aerogels. Several methods are employed to characterize the annealed $(Ru-Ti)O_x$ aerogels. X-ray diffraction (XRD) is used to determine the presence and identity of crystalline phases in the aerogels. The Scherrer formula is used to estimate the size of the crystalline domains. The surface properties and composition of the aerogels are examined using X-ray photoelectron spectroscopy (XPS, Fisons 220iXL, monochromatic Al Kα X-rays). Single-point nitrogen adsorption (BET) measurements (Quantachrome Monosorb) with 30% N_2/He are used to measure surface areas within ±10%. Atomic absorption spectroscopy (Corning Analytical Laboratory) of the digested solids indicates a bulk composition of $Ru_{0.32}Ti_{0.68}O_x$. The density of the aerogels is determined from their displacement of mercury in a Moore−Van Slyke specific gravity bottle.

For impedance measurements, the $(Ru-Ti)O_x$ aerogels are ground into a fine powder using a mortar and pestle and then hand-pressed into a 0.05-cm-thick disk using a 0.4-cm diameter die. The resulting pellets are ∼20% of the theoretical density of 32 mol % RuO_2-TiO_2. They appear uniform in thickness and exhibit excellent mechanical integrity. Although electrical measurements of porous materials are inherently compromised,[39,40] we normalize most of the variables by using samples of approximately the same weight and thickness and then assume a constant geometric ratio, L, of 3 cm based on the radius and average thickness of the samples ($L = A/d$, where A is the geometric electrode area and d is the distance between the electrodes). In this way it is possible to determine the relative differences between the conductivities of porous materials. Similar methodology has been successfully used elsewhere to study metal oxide powders.[41,42] The BET surface-area measurements show that our method of grinding and pressing the aerogel powder does not decrease the surface area accessible to gas adsorption and, in several cases, resulted in an effectively larger surface area.

Two-probe impedance measurements are executed using a frequency response analyzer (Solartron 1260) at frequencies between 10 and 10^7 Hz. The (Ru+Ti)oxide aerogel pellets are spring-loaded between platinum leads in an alumina cell and loaded into a quartz tube so that the sample can be exposed to different gas flows and temperatures. Gold blocking electrodes were sputtered on some aerogel pellets to ensure even electrical contacts, but these contacts only modestly affected the interfacial impedance and had little influence on the bulk conductivity. Therefore, blocking electrodes are not necessary in these electrical measurements. A commercial impedance spectroscopy package (Scribner Associates Z60/ZView/ZPlot) is used to collect and analyze the data. The sample resistance, R, is determined from a least-squares analysis of the complex impedance. The electrical conductivity, σ, is calculated using the equation $\sigma = 1/RL$.

Preparation and Annealing of TiO_2 Aerogels. For comparison to the $(Ru-Ti)O_x$ aerogels, TiO_2 aerogels have been prepared using the unmodified literature preparation[36] and the above procedures. The reactant ratios used in these standards are shown in Table 1. The gels appear clear after gelation and crack upon submersion in acetone. Over time, the gels become brown in the acetone indicating the oligomerization of acetone on their surfaces. After they are dried under supercritical CO_2, the gels are heated in ambient air at 2 °C/min to 460 °C and annealed for 5 min before cooling at 2 °C/min. These TiO_2 aerogels are characterized as described above for $(Ru-Ti)O_x$ aerogels.

(37) Drying the ethanol over molecular sieves (zeolite 4A, UOP) yields aerogels that are visibly nonuniform, presumably due to salts introduced into the ethanol (and thereby into the sol−gel chemistry) by zeolite-induced autoprotolysis of trace water in the ethanol.

(38) Kristóf, J.; Liszi, J.; DeBattisti, A.; Barbieri, A.; Szabó, P. *Mater. Chem. Phys.* **1994**, *37*, 23.

(39) Macdonald, J. R., Ed. *Impedance Spectroscopy: Emphasizing Solid Materials and Systems*; John Wiley and Sons: New York, 1987.

(40) Raistrick, I. D. *Solid State Ionics* **1986**, *18/19*, 40.

(41) England, W. A.; Cross, M. G.; Hamnett, A.; Wiseman, P. J.; Goodenough, J. B. *Solid State Ionics* **1980**, *1*, 231.

(42) Dzimitrowicz, D. J.; Goodenough, J. B.; Wiseman, P. J. *Mater. Res. Bull.* **1982**, *17*, 971.

Results and Discussion

Characterization Prior to Annealing. The formation and structure of the (Ru−Ti) gels are highly dependent on the sol−gel chemistry. The gelation time of the sol, which is a measure of the kinetics of the gelation process, increases with increasing Ru content, decreasing acid content, and decreasing water content (Table 1). Once gelled, the stiffness of the gels increases with increasing initial water concentration, but precipitation occurs in the solutions when the water-to-metal molar ratio exceeds 6. Gels made with a metal-to-acid molar ratio of 1:0.08 (gels A and C) exhibit greater physical integrity than those with a ratio of 1:0.12 (gels B and D).

The gelation kinetics are also affected by the nature of the $RuCl_3$ precursor. The time of gelation varies by more than an order of magnitude (e.g., 3 min to 3 h) when a different source or batch of $RuCl_3$ is used. XRD shows that anhydrous $RuCl_3$ purchased from Alfa ($RuCl_3$ [Alfa]) is α-$RuCl_3$ with a RuO_2 impurity phase, while that from Aldrich ($RuCl_3$ [Aldrich]) has a crystalline structure that could not be identified in sets 1−43 of the JCPDS data base (International Centre for Diffraction Data). The phase of $RuCl_3$ [Aldrich] varied in different batches.

XPS analysis of the chemical state of the chlorine and oxygen in these commercial sources of $RuCl_3$ confirms the difference in their structure and chemistry. $RuCl_3$ [Alfa] has one type of chlorine species, consistent with chloride ion, while $RuCl_3$ [Alrich] has a second distinct Cl 2p peak and, therefore, an additional type of chlorine. The second chlorine state in the $RuCl_3$ [Aldrich] resembles that observed in amorphous $RuCl_3$ hydrate ($RuCl_3 \cdot 1-3H_2O$, Aldrich). On the basis of these XPS and other TGA data, $RuCl_3$ [Aldrich] consists primarily of a partially hydrated form of $RuCl_3$. $RuCl_3 \cdot yH_2O$ is inherently difficult to characterize, because it undergoes varying degrees of hydration and polymerization and hosts several different oxidation states of Ru.[43] Therefore, $RuCl_3 \cdot yH_2O$ cannot be used reliably as a known, chemically unique precursor for sol−gel chemistry.

The difference in the nature of the commercial $RuCl_3$ precursors is also apparent when the sol−gels are washed in acetone. When $RuCl_3$ [Alfa] is used, the acetone from the first two washes is clear but subsequently appears pale green, indicating the loss of some Ru-containing species from the gel into the acetone. In gels made from $RuCl_3$ [Aldrich], up to 50% of the Ru leaches out during the first two acetone washes.

Gels made from both $RuCl_3$ precursors remain monolithic after washing in acetone. These gels crack slightly and lose ca. 25% of their original volume during supercritical drying. The amount of cracking can be reduced by heating and cooling the gels slowly (e.g., 2 °C/min) during the supercritical drying process. The unannealed aerogels derived from $RuCl_3$ [Alfa] are black; XRD reveals that particles of α-$RuCl_3$ are present. When $RuCl_3$ [Aldrich] is used, the aerogels are light or dark brown and are amorphous to X-rays.

TGA indicates that the pyrolysis of chloride and alkoxides from $RuCl_3$ [Alfa]-derived aerogels occurs by 410−420 °C under wet Ar (Figure 1). Little weight is gained while cooling under O_2/H_2O from 410 to 50 °C, suggesting that $(Ru-Ti)O_x$ is not severely reduced during the Ar/H_2O thermal treatment. By increasing the heating rate from 2 to 5 °C/min, temperatures up to 60 °C higher are needed to evolve the alkoxide and chloride components of the gels. In aerogels derived from the $RuCl_3$ [Aldrich] precursor, this weight loss occurs at lower temperatures, i.e., 350 °C under wet Ar.

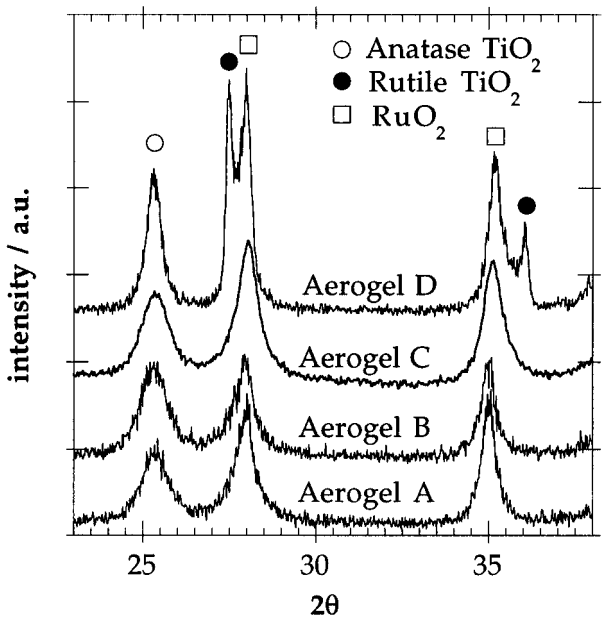

Figure 2. Variations in the crystalline portion of the $(Ru-Ti)O_x$ aerogel series of Table 1 as measured by XRD after heating aerogels A−D to 410 °C in Ar/H_2O and cooling under O_2/H_2O.

During annealing, the $(Ru-Ti)O_x$ aerogels further densify to about 50% of the initial volume of the wet gels. The final aerogels retain a cracked monolithic form and are colored gray or black. The densities of the monolithic annealed $(Ru-Ti)O_x$ aerogels are ∼12% of the theoretical density of 32 mol % RuO_2-TiO_2. In comparison, the pure TiO_2 aerogels as made are more extensively cracked and transform to a white powder during annealing.

Characterization of Annealed Aerogels. *Physical Properties.* After annealing, XRD indicates that the $(Ru-Ti)O_x$ aerogels contain crystalline portions of TiO_2 and RuO_2, as shown in Figure 2 for the aerogels prepared from the chemistries in Table 1. The crystalline fraction of aerogels A, B, and C correspond to anatase TiO_2 and rutile RuO_2, while aerogel D contains both anatase and rutile forms of TiO_2 as well as rutile RuO_2. On the basis of the Scherrer formula, the peak widths indicate that these crystallites are ∼10 nm in diameter. The TiO_2 aerogels have an anatase structure with 10-nm crystallites.

The relative XRD peak intensities of the anatase TiO_2 and the rutile TiO_2 and RuO_2 vary in the $(Ru-Ti)O_x$ aerogels, even though they have an equal concentration of Ru and were annealed under identical conditions. A possible explanation of this variation is incomplete crystallization[14] of the initially amorphous aerogel. Because of the relatively low annealing temperatures,

(43) Seddon, E. A.; Seddon, K. R. *The Chemistry of Ruthenium*; Elsevier: Amsterdam, 1984.

(44) Merzbacher, C. I.; Swider, K. E.; Rolison, D. R. Abstract V5-22, MRS 1996 Fall Meeting, 2−6 Dec 1996, Boston, MA; Materials Research Society: Pittsburgh, PA, 1996; p 519.

solid-state diffusion is minimized and the initial sol−gel chemistry primarily controls the final aerogel structure. Small-angle neutron-scattering studies are also being pursued to characterize further the nanoscale structure of $(Ru-Ti)O_x$ aerogels.[44]

The average surface area of aerogels A−D is 85 ± 15 m^2/g. For aerogels with the molecular formula of $Ru_{0.32}Ti_{0.68}O_2$, this yields a molar surface area of 9880 (±1450) m^2/mol. Our TiO_2 aerogels have an average surface area of 110 ± 5 m^2/g or ca. 8800 m^2/mol of TiO_2. TiO_2 aerogels made from chemistries similar to those in Table 1 and annealed at 400−500 °C have surface areas of 65−128 m^2/g,[36] or molar surface areas of 5190−10 200 m^2/mol. Therefore, the addition of Ru to this Ti sol−gel chemistry[36] does not result in a decrease in surface area.

The surface analysis of the $(Ru-Ti)O_x$ aerogels by XPS consistently indicates that little residual chlorine (e.g., <1 atom %) remains after annealing. The analysis of the Ru 3d, Ti 2p, and O 1s regions obtained for these aerogels is not straightforward. The aerogels from the A−D series react in situ with the X-ray beam in UHV, and their spectra vary as a function of time, shifting to more anhydrous RuO_2-like with increased X-ray exposure. This is contrary to the typical effects of beam damage, wherein photoelectron reduction of metal oxides is usually observed.[45] The $(Ru-Ti)O_x$ aerogel surfaces measured with XPS are therefore not necessarily representative of their state in ambient atmospheres.

Electrical Properties. Although RuO_2 is a known electronic conductor, proton conduction due to adsorbed surface water must also be considered in low-temperature electrical measurements of all oxides.[2] Proton conduction occurs along the surfaces of oxides usually by a mixed-translocation mechanism, whereby the H^+ or H_3O^+ ions conduct along a hydrous, "liquidlike", water structure adsorbed on the charged oxide surface.[2,41] This general mechanism has been used to describe the protonic conduction observed on the hydrous surfaces of many transition-metal and rare-earth oxides, including V_2O_5, SnO_2, ZrO_2, Sb_2O_5, In_2O_3, Cr_2O_3, Ga_2O_3, Ta_2O_5, Nb_2O_5, CeO_2, and ThO_2.[2,27,41,42,46] The amount of adsorbed water is a function of the charging, or acidity, of the oxide surface which in turn depends on the cations, structure, and particle size of the oxide.[2,41]

Dense polycrystalline metal oxides (contacted with nonblocking electrodes) have four dominant proton conduction regimes that can be measured with impedance spectroscopic measurements (Figure 3a): [1] within the lattice or bulk; [2] the surfaces in series with crystals; [3] the surfaces in parallel with crystals; [4] the interfacial impedance of the solid with the atmosphere or a nonblocking electrode.[2,39−41] This model can be expressed using the equivalent circuit shown in Figure 4a. In this figure, $R_{H^+}(1)$ is a resistor representing protons conducting in the oxide lattice (e.g., interstitial protons). Resistors also represent the conduction paths along the surfaces in series, $R_{H^+}(2)$, and in parallel, $R_{H^+}(3)$, with the crystals. The electrical circuit of these three paths is in series with the interfacial resistance of the protons, $R_{H^+}(4)$. The movement of protons in each region of the material has an associated capacitance represented by C_1, C_2, etc.

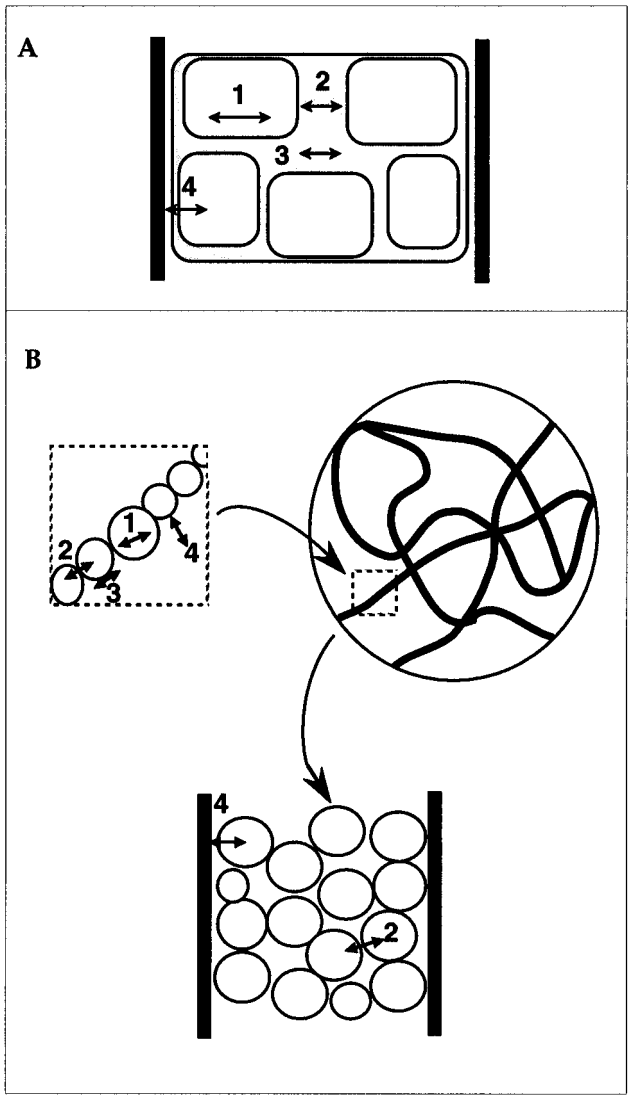

Figure 3. (a) The four conduction domains in polycrystalline materials: [1] the crystalline lattice, [2] the surfaces in series with crystals, [3] the surfaces in parallel with the crystals, and [4] the interface between the polycrystals and the atmosphere or electrodes. (b) The four conduction domains in aerogels: [1] within the crystalline particles, [2] the interface of the surfaces between two particles, [3] the surface along the particles, and [4] the interface between the particles and the atmosphere or electrodes.

A schematic of the conduction regions in an aerogel is shown in Figure 3b. In this nanoscale, meso- and microporous material, conduction also occurs in four regions: [1] within nanoscale particles; [2] between adjacent nanoscale particles; [3] along the surfaces of the particles; [4] at the interface of the aerogel particles with the electrical contacts and the atmosphere. These regions are analogous to those used to describe proton conduction in dense polycrystalline oxides, and so the equivalent circuit in Figure 4a can also be used to describe conduction in high-surface-area aerogels.

The impedance, Z, of an equivalent circuit is the sum of its circuit elements. As with resistors, impedance elements in series are added, whereas the inverse impedance is added for elements in parallel. The impedance of a resistor and capacitor in parallel is

(45) Powell, C. J.; Seah, M. P. *J. Vac. Sci. Technol. A* **1990**, *8*, 735.
(46) Barboux, P.; Baffier, N.; Morineau, R.; Livage, J. *Solid State Ionics* **1983**, *9/10*, 1073.

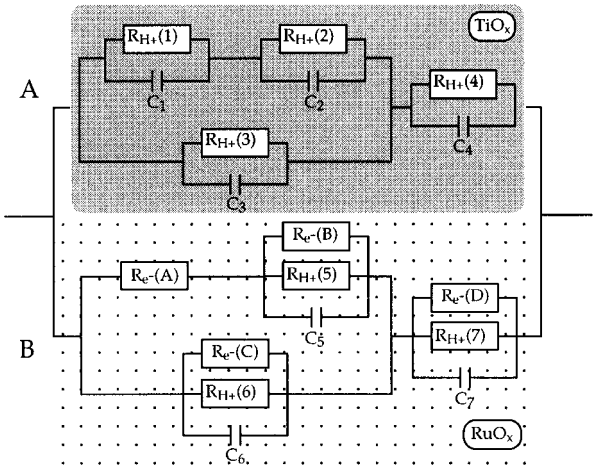

Figure 4. (a) Equivalent circuit representing protonic conduction in the TiO_2 lattice [$R_{H^+}(1)$], surface layers [$R_{H^+}(2)$ and $R_{H^+}(3)$], and the interface of the surface with the atmosphere and electrodes [$R_{H^+}(4)$]. Protonic conduction in all four regions has an associated capacitance, C_1, C_2, C_3, C_4. (b) Equivalent circuit representing mixed electronic/protonic conduction in RuO_x: electronic conduction in the RuO_x lattice [$R_{e^-}(A)$] and hydrous surface layer (domains 2 and 3 in Figure 3b) [$R_{e^-}(B)$ and $R_{e^-}(C)$], and protonic conduction in the RuO_x hydrous surface layer [$R_{H^+}(5)$ and $R_{H^+}(6)$]. $R_{e^-}(D)$ and $R_{H^+}(7)$ represent mixed conduction at the hydrous RuO_x−electrode interface. The proton conduction at the surfaces and interfaces have associated capacitances: C_5, C_6, C_7.

written in complex notation as a function of frequency, ω, in eqs 1 and 2:

$$\frac{1}{Z} = \frac{1}{R} + i\omega C \tag{1}$$

$$Z = \frac{R}{1 + \omega^2 R^2 C^2} - i\frac{\omega R^2 C^2}{1 + \omega^2 R^2 C^2} \tag{2}$$

When the capacitances associated with each conduction region differ by several orders of magnitude (e.g., $C_1 \ll C_2$), the impedance of each conduction region separates into a distinct semicircle in the complex impedance plane (Z_{real} versus Z_{imag}).

The complex impedance of a pressed pellet of TiO_2 aerogel at room temperature is shown in Figure 5. One broad semicircle is measured, which suggests one dominant ionic conduction process. Protonic conduction is expected only along the surface as the concentration and room-temperature mobility of interstitial protons in TiO_2 is low.[2] Because $R_{H^+}(1)$ is very large relative to the other three conduction paths, $R_{H^+}(3)$ can be approximated from the intercept of the semicircle with the real impedance axis (Z_{real})[39,47] to be 1.5×10^8 Ω. Using a geometric ratio of 3 cm, this correlates to a conductivity of 2×10^{-9} S cm^{-1}. The semicircle is distorted, presumably due to a distribution in the grain sizes in the TiO_2 aerogel, but this fitting method is still valid.[47] The interfacial response, $R_{H^+}(4)$, is beyond the detection limit of our frequency response analyzer.

The presence of water on the TiO_2 aerogel is confirmed by TGA measurements which show that 6 wt % of the sample is lost between 25 and 400 °C under dry Ar, corresponding to a molar formula of $TiO_2 \cdot 0.28H_2O$. Approximately half of the weight loss occurs below 50 °C, consistent with physisorbed water. The remainder of the weight loss can be attributed to the loss of both physisorbed and chemisorbed water. As expected for a surface proton conductor, an increase of water vapor in the atmosphere decreases the resistance of the TiO_2 aerogel. As seen in Figure 5, the resistance decreases after only 5 min of exposure to wet Ar gas. After 5 h of exposure to wet Ar, the resistance of the TiO_2 aerogel drops by 2 orders of magnitude, corresponding to a proton conductivity of 1×10^{-7} S cm^{-1}. Under very humid atmospheres, Warburg impedance is observed which is expected as the concentration of physisorbed water increases, and the proton conduction changes from the translocation or hopping mechanism to a diffusion-controlled mechanism.

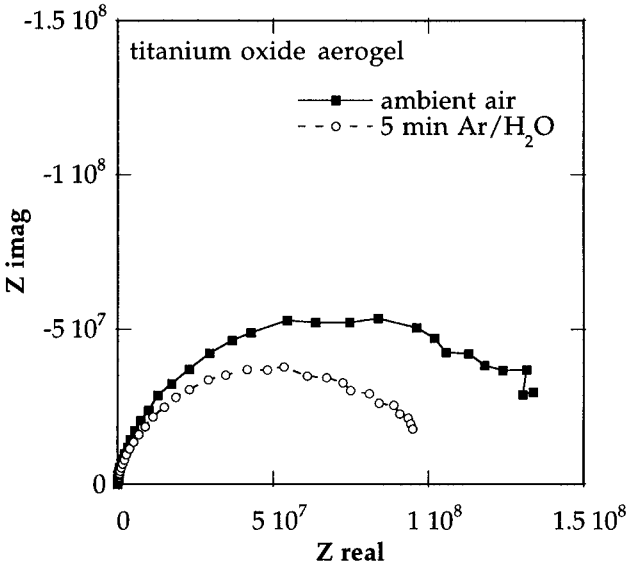

Figure 5. Complex impedance of proton conduction in a TiO_2 aerogel in air and under wet Ar.

In other (Ru−Ti)O_x aerogels prepared in our laboratory, we observe that the addition of less than 20 at. % Ru for Ti has little effect on the conductivity of (Ru−Ti)O_x aerogels relative to pure TiO_2 aerogels, presumably because the concentration of the ruthenium oxide in these porous materials is below the percolation threshold for conduction. However, the $Ru_{0.32}Ti_{0.68}O_x$ aerogels from Table 1 exhibit a marked change in the impedance response from the pure TiO_2 aerogels, as shown in Figure 6. The frequency response of these (Ru−Ti)O_x aerogels also has a capacitive component, indicating that the resistivity is not purely electronic, as would be expected for a bulk 32 mol % RuO_2−TiO_2 material.[14] Therefore, this electrical response must be attributed to a protonic conduction process.

Because the resistivity of the $Ru_{0.32}Ti_{0.68}O_x$ aerogel is 4 orders of magnitude lower than that of the TiO_2 aerogel, it is best explained by a second proton conduction process that occurs in parallel to the TiO_2 or along the RuO_x surface. A model for the electrical conduction paths in a mixed-conducting RuO_2 is shown in parallel with the TiO_2 in the equivalent circuit in Figure 4b. The electronic conduction in the RuO_2 bulk is represented by one resistance element, $R_{e^-}(A)$; although electrons may conduct by either the d-bands of the oxide or by hopping between Ru^{3+} and Ru^{4+}, the latter mechanism is unlikely at room temperature. This electronic conduction is in series and parallel with proton conduction

(47) Armstrong, A. D.; Dickinson, T.; Willis, P. M. *J. Electroanal. Chem.* **1974**, *53*, 389.

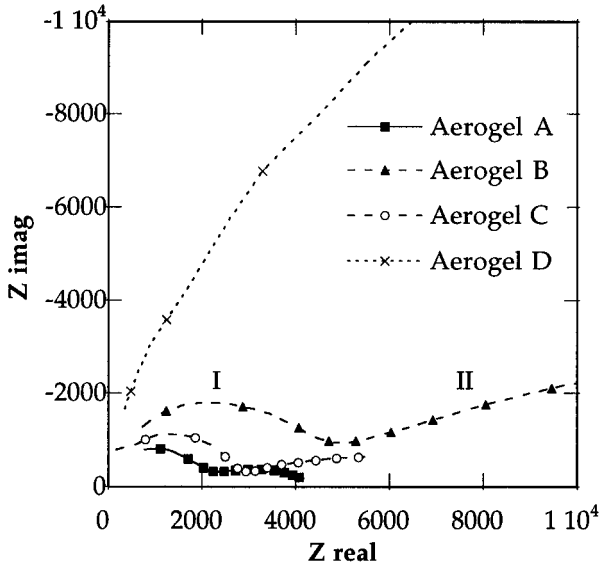

Figure 6. Complex impedance of proton conduction in (Ru−Ti)O_x aerogels A−D. Semicircle I results from the impedance of the hydrous surface layer, and II is caused by that of the electrode interface.

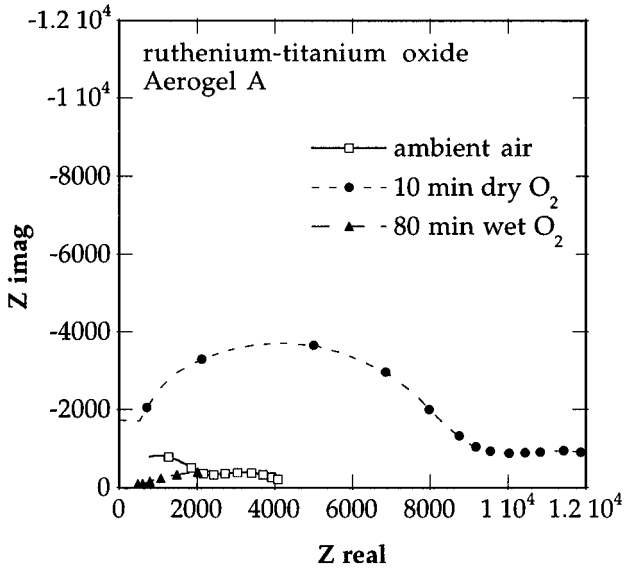

Figure 7. Effect of atmospheric water pressure on the complex impedance of (Ru−Ti)O_x aerogel A.

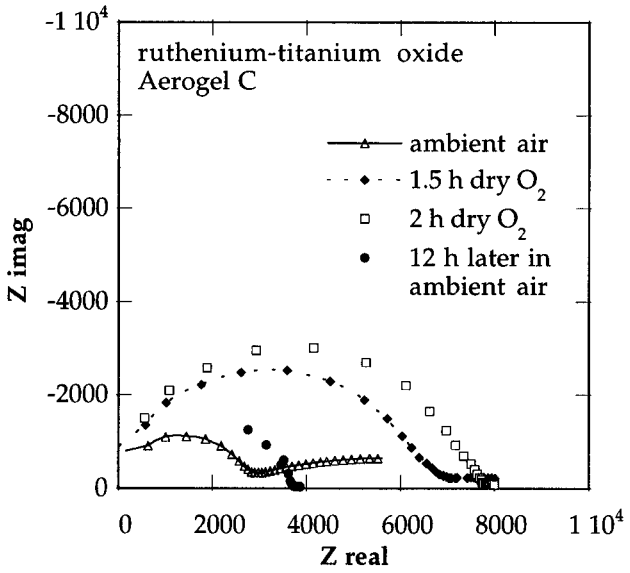

Figure 8. Complex impedance of (Ru−Ti)O_x aerogel C with extended exposure to dry O_2.

paths along a hydrous ruthenium oxide surface (whereby the term hydrous designates RuO_xH_y, $Ru(OH)_x$, $RuO_2 \cdot yH_2O$, etc.). Hydrous ruthenium oxide is an electronic conductor[13] but should conduct protons similarly to other hydrous transition-metal oxides.[2,3,6,40,41,46] Therefore, on the hydrous ruthenium oxide surface, both electrons [R_{e^-}(B) and R_{e^-}(C)] and protons [R_{H^+}(5) and R_{H^+}(6)] conduct in parallel. Similarly, the ruthenium oxide at the interface with the atmosphere and electrodes should be hydrous and have both electronic, R_{e^-}(D), and protonic, R_{H^+}(7), components.

On the basis of the above model for a series of electronically conducting RuO_2 particles in series and in parallel with mixed-conducting hydrous ruthenium oxide surfaces, the left semicircle (arc I) in Figure 6 can be attributed to surface conduction and the right half-circle (arc II) is due to the interface of the sample with the atmosphere and the electrodes of the conductivity cell.[41,42] Electronic conduction in the RuO_2 lattice cannot be detected because it has no frequency dependence and it is in series with the higher resistivity of protons at the surface. Fitting arc I of aerogels A, B, and C indicates that their resistance is 2000−5000 Ω ($\sigma = 2 \times 10^{-4}-7 \times 10^{-5}$ S cm^{-1}). The impedance response of aerogel D is only partially shown in Figure 6, because its resistance is 40 000 Ω.

The surface protonic contribution to the impedance response of the (Ru−Ti)O_x aerogels is confirmed by the water-pressure dependence of the resistance. As observed with the TiO_2 aerogels, the resistance becomes higher when the sample is exposed to dry gas (e.g., O_2, Ar, H_2) and decreases with an increase in the water pressure of the atmosphere (Figure 7). Warburg impedance can also be observed after extended exposure to a humid atmosphere. The electrical resistance increases when (Ru−Ti)O_x aerogels are heated to 100 °C, as is expected when a protonic conductor loses surface water. TGA shows that during heating to 400 °C under dry Ar, the weight of aerogels A, B, C, and D decreases on average by 4.5%, indicating that the molar formula of the aerogel is $Ru_{0.32}Ti_{0.68}O_x \cdot 0.25H_2O$ at room temperature in air. The weight-loss profiles of the (Ru−Ti)O_x aerogels are similar to those observed for TiO_2 aerogels.

The capacitive component to arc II indicates that the interfacial conduction of the (Ru−Ti)O_x aerogels is also governed by protons and that the metal electrodes of the conductivity cell act as partial blocking electrodes. This interfacial impedance is eliminated by exposing the aerogel to dry O_2 for over 2 h (Figure 8). The loss of contact resistance at the electrode/aerogel interface is confirmed with two-probe dc resistance measurements with a multimeter (Keithley 179A). The dc resistance is within 20 Ω of the ac resistance (i.e., the intercept of arc I with Z_{real}). The interfacial resistance is not eliminated when (Ru−Ti)O_x aerogels are exposed to wet rather than dry O_2.

Defect equilibria for RuO_2 can be used to explain these conductivity results. Using Kröger−Vink notation,[48] the effect of oxygen and water partial pressures on the RuO_2 structure is written as follows:

(48) Kröger, F. A. *The Chemistry of Imperfect Crystals*; Elsevier: New York, 1974; Vol. 2, p 14.

$$2Ru_{Ru}' + V_O^{\bullet\bullet} + {}^1/_2O_2(g) \leftrightarrow 2Ru_{Ru} + O_O \quad (3)$$

$$2OH_O^{\bullet} \leftrightarrow O_O + V_O^{\bullet\bullet} + H_2O(g) \quad (4)$$

$$2Ru_{Ru}' + 2OH_O^{\bullet} + {}^1/_2O_2(g) \leftrightarrow 2Ru_{Ru} + 2O_O + H_2O(g) \quad (5)$$

In these equations, Ru_{Ru} represents a Ru^{4+} cation on a 4^+ cation site in the RuO_2 lattice, and Ru_{Ru}' corresponds to a Ru^{3+} cation on the same Ru site, resulting in an effectively negative charge (′) in the lattice. Similarly, O_O is an oxygen ion in the RuO_2 lattice, $V_O^{\bullet\bullet}$ is an effectively positive oxygen vacancy, and $OH_O^{\bullet}$ represents an oxygen−proton complex on an oxygen site.

Equation 3 indicates that an increase in oxygen pressure can shift the Ru oxidation state from Ru^{3+} to Ru^{4+}. This reaction is accompanied by the consumption of $V_O^{\bullet\bullet}$. Because the mobility of vacancies is low at room temperature, the reaction is limited to the ruthenium oxide surface. On the hydrous ruthenium oxide surface, $V_O^{\bullet\bullet}$ may become occupied by water, as expressed in eq 4. Upon a decrease in the water pressure, $V_O^{\bullet\bullet}$ forms. The sum of these oxygen and water equilibria, written in eq 5, can be used to explain the conductivity results shown in Figure 8. The increase in oxygen pressure and decrease in water pressure which occurs when the (Ru−Ti)O_x aerogel is exposed to dry O_2 results in the formation of more Ru^{4+}, or RuO_2, on the aerogel surface, leading to an increase in its electronic conductivity and a decrease in the electrode contact impedance.

The protonic conduction on the surfaces of the aerogel network persists despite extended exposure to oxygen. The surface resistance is higher under dry O_2 than wet O_2 (Figure 8), presumably due to the loss of surface water. The electronic conduction at the oxidized surface unfortunately cannot be resolved from the impedance data due to the complexity of the system, as expressed by the equivalent circuit in Figure 4. These results suggest that high electronic conduction cannot be achieved at the aerogel surfaces, because they are comprised of a highly defective hydrous ruthenium oxide or (Ru−Ti)O_x. These electronically insulating surfaces separate the crystalline RuO_2 regions in the aerogels, so that the electronic conductivity does not short-circuit through the material, as occurs in bulk RuO_2−TiO_2.

Conclusions

When RuO_2−TiO_2 is expressed as an aerogel, its electrical properties are controlled by its surface conductivity which arises from proton conduction in a hydrous ruthenium oxide layer. The electronic conductivity, which dominates the electrical properties of bulk RuO_2−TiO_2, is disrupted in the nanoscale material such that its protonic conductivity can be measured despite the presence of RuO_2 and TiO_2 nanoscale phases. This finding suggests that the bulk properties which have been reported for RuO_2−TiO_2 are misleading to those researchers interested in its catalytic and capacitive nature, because the actual surface of the material is mixed-conducting and most likely has the formula $Ru_nTi_{1-n}O_xH_y$.

Preparing transition-metal oxides in the nanoscale mesoporous form of aerogels provides a unique opportunity to characterize surface properties that are otherwise difficult to isolate in the bulk or colloidal state. This opportunity is countered by an intriguing dichotomy for the electrically conducting aerogels, i.e., the hydrous oxide surface, which controls the electrical transport properties in the aerogel, cannot be characterized by many standard materials characterization techniques (e.g., diffraction). Yet probing hydrous oxide layers by surface-sensitive measurements will need to be done without inducing artifactual information by altering the nature of the hydrous oxide in unknown or uncontrolled manners. This dichotomy will need to be considered as these and other electrically conductive transition-metal oxide aerogels are synthesized, characterized, and applied as electrical and electrochemical materials.

Acknowledgment. This work was supported by grants from the Office of Naval Research and DARPA. We are grateful to Prof. Bruce Dunn (UCLA) for catalyzing our introduction to aerogel synthesis and to Robert Bernstein (Physical Science Aid, NRL-Alfred University Co-operative Research Program) for assistance in obtaining the TGA and XRD analyses of our samples. K.E.S. would like to thank the American Society for Engineering Education for support of her postdoctoral fellowship (1993−1996).

CM960622C